Variability and degradation of homeostasis in self-sustained oscillators

Wright, T., Twaddle, J., Humphries, C., Hayes, S. & Kim, E. J.

DOI 10.1016/j.mbs.2016.01.002
ISSN 0025-5564

Publisher: Elsevier

Variability and degradation of homeostasis in self-sustained oscillators

Thomas Wright, James Twaddle, Charlotte Humphries, Samuel Hayes and Eun-jin Kim*

School of Mathematics and Statistics,

University of Sheffield, Sheffield, S3 7RH, UK

Abstract

Homeostasis is known to be absolutely critical to the sustainability of living organisms. At the heart of homeostasis are various feedback loops, which can control and regulate a system to stay in a most favourable stable state upon the influence of various disturbance. While variability has emerged as a key factor in sustainability, too much variability could however be detrimental. It is thus absolutely crucial to understand the effect of fluctuation in different feedback loops. Despite a great advancement in modelling technique, this issue is far from being understood completely as too a complicated model often prevents us from disentangling many different processes.

Here, we propose a novel model to gain a key insight into the effect of variability in feedback on self-sustained oscillation. Specifically, by taking into account variation in model parameters for self-excitation and nonlinear damping, corresponding to positive and negative feedback, respectively, we show how fluctuation in positive or negative feedback weakens the efficiency of feedback and affects self-sustained oscillations, possibly leading to a complete breakdown of self-regulation. While results are generic and could be applied to different self-regulating systems (e.g. self-regulation of neuron activity, normal cell growth, etc), we present a specific application to heart dynamics. In particular, we show that fluctuation in positive feedback can lead to slow heart by either amplitude death or oscillation death pathway while fluctuation in negative feedback can lead to fast heart beat.

* Corresponding author: e.kim@shef.ac.uk

I. INTRODUCTION

Homeostasis is known to be absolutely critical to the sustainability of living organisms (e.g. [1]). Simply put, it means 'not too much, not too little, but just right.' More technically, it represents the ability of a system, which can control and regulate itself to stay in a most favourable stable state upon the influence of various disturbance. This is entailed by the presence of two (or more) opposing and complementary forces (or requirements) in a system and by the adjustment of these forces when perturbed to restore a subtle balance through different positive or negative feedback loops. Self-regulation breaks down when a system is no longer under the control of such feedback mechanism, e.g., when one of the forces is overpowered by the other. For instance, normal cells have the ability of self-regulating their growth by maintaining the balance between growth and death, and its breakdown can lead to the overgrowth of cells and consequently tumour cells. Tumour cells can thus result not only from the loss of the ability of inhibiting growth (e.g. the loss of tumour suppressor genes) but also from the activation of uncontrolled growth factor (e.g. the activation of oncogenes) [2]. Another interesting example is self-regulation of neural activity where the balance between excitatory and inhibitory neurons is crucial for the maintenance of normal function of neuron. Either over-excitation of excitatory neuron or under-activation of inhibitory neuron can lead to abnormal brain activity such as eclipse [3]. One more, but not the last, example would be normal function of heart and heart rhythm as a result of self-regulation, and this will be of our main focus regarding application of our results in this paper. With myriad of similar examples found in living organisms, self-regulation – a fundamental feature of homeostasis – is also at the heart of the emergence and maintenance of self-organised structures in many other complex systems, including large-scale flows, magnetic fields, and vortices in astrophysical and laboratory fluids, environments, and chemical reactions (e.g. see [4–8]).

Our work is motivated to understand how homeostasis is affected when one of feedback loops becomes less effective due to fluctuation. While this can be caused by the intrinsic problem with chemical, biological, or physiological process itself (e.g. ion channels, gene expression, tissue damage, etc), it also seems to be an inevitable consequence of a system involving multi-scale processes where fluctuation arises not only from the inhomogeneity and heterogeneity in the system but also from the environmental influence. In view of emerging evidence of variability and fluctuation and their relevance in many systems [5–13], it is timely to undertake a systematic investigation of this issue and quantify the effect of fluctuations in different feedback loops in a self-sustained oscillator.

To this end, we revisit the Van der Pol oscillator and study the effect of fluctuations in the model parameters for positive and negative feedback due to self-amplification and nonlinear damping, respectively. We introduce our model in Section II. Section III reports on the effect of modulation in self-amplification. Section IV presents the results on the modulation in nonlinear damping and the loss (i.e. degradation) of self-regulation. Section V discusses implications for heart dynamics. Conclusion and discussion are provided in Section VI. Appendices include linear stability analysis and application to heart dynamics. We note that Sections III and IV contain rather detailed mathematical analysis, and readers who are mainly interested in applications are welcome to go to Section V after skimming through Section II.

II. MODEL

The Van der Pol oscillator is a prototypical mathematical model for self-sustained oscillations. Since originally proposed by Van der Pol to understand oscillations in nonlinear electric circuits, it has been developed further to investigate human heart and the stability of heart dynamics [14–24] and extended to different disciplines (e.g. biology, fluids, environments, engineering) [25]. This model is described by the following ordinary differential equation (ODE):

$$\frac{d^2x}{dt^2} + (-\alpha + \beta x^2)\frac{dx}{dt} + \omega_0^2 x = 0. \tag{1}$$

Here, α and β are control parameters which represent the efficiency of amplification and nonlinear damping, respectively; ω_0 is the natural frequency at which a system in the absence of the amplification and damping (e.g. when $\alpha = \beta = 0$) oscillates. The term $-\alpha\frac{dx}{dt}$ with $\alpha > 0$ leads to exponential growth of a linear solution while the term $\beta x^2\frac{dx}{dt}$ with $\beta > 0$ due to nonlinear damping limits the growth to a finite value [35]. Therefore, in regards to self-regulation mentioned previously, α and β represent the efficiency of positive and negative feedback, respectively. When a system is well self-regulated, self-amplification and nonlinear damping act together in balance, and lead to self-sustained relaxation oscillation as a limit cycle. This is modelled by using constant positive values for α and β. However, when there is some dysfunction in either positive or negative feedback loop (see §IV for further discussion), its efficiency is reduced, causing a mismatch between the two such as time delay in balance. We model this inefficiency in either feedback by including a time-varying part in α or β, respectively. As noted in Section I, in continuous systems, Eq. (1) is a mean-field equation for the time-evolution of large-scale observables while control parameters capture the overall effect of unresolved small-scale dynamics.

To gain a key insight into the effect of fluctuations in α and β, we, for simplicity, take α and β to consist of constant and periodic modulation parts as follows:

$$\alpha = \mu_1 + \epsilon_1 \sin(\omega_1 t), \quad (2)$$

$$\beta = \mu_2 + \epsilon_2 \sin(\omega_1 t). \quad (3)$$

Here, μ_1 and μ_2 are constant parts; ϵ_1 and ϵ_2 are the amplitude of the modulation while ω_1 is the angular frequency of the modulation [36]. By using the unit where the natural frequency $\omega_0 = 1$ (see later), and by varying values of μ_1, μ_2, ϵ_1, ϵ_2, and ω_1, we investigate how fluctuation in α and β affects the bahaviour of self-sustained oscillation. As our main purpose is to gain a key insight into implications for homeostasis (heart dynamics), we focus on qualitative behaviour of bifurcations upon the change of parameters, leaving a more detailed study on bifurcation sequence for future work. We explore the possibility of the breakdown of self-regulation and highlight a crucial role of efficient feedback in sustainability.

We should note that for nonlinear oscillators, the effect of fluctuations has been studied previously by many authors where fluctuations appear as multiplicative or additive noise. In particular, much attention has been paid to the case when natural frequency ω_0 contains a random part, with a strong interest in parametric instability or stochastic resonance. In contrast, the effect of fluctuation on parameters α and β has been studied much less (e.g. see [26]), which will be the focus of this paper. Also, in the case of the Van der Pol oscillator, the periodic additive forcing has been shown to lead to devil's staircase with chaos sandwiched between two nearby period doublings (e.g. see [27]). In the following, we show that similar devil's staircase also results from multiplicative noise.

III. FLUCTUATION IN POSITIVE FEEDBACK: $\alpha = \mu_1 + \epsilon_1 \sin(\omega_1 t)$, $\beta = 1$

To understand the effect of periodic modulation in α, it is useful first to examine its effect on linear oscillation in the absence of nonlinear damping term (i.e. $\beta = 0$) in Eq. (1). As detailed in Appendix A, fluctuation in α can help a linear solution grow exponentially [37]. In the case of a purely periodic $\alpha = \epsilon_1 \sin \omega_1 t$, the onset of linear instability occurs when the amplitude of ϵ_1 is sufficiently large. The critical value of ϵ_1 for the onset of linear instability depends on ω_1, μ_1 and the frequency p of excited mode. In general, a larger critical ϵ_1 is needed as μ_1 and ω_1 increase. This is shown in Appendix A where a linear dispersion relation is derived by keeping the interaction of the two adjacent modes, which are coupled through the periodic modulation. Resonant interaction excites the following two types of modes of $p_A = \omega_1/2$ and $p_B = \sqrt{\frac{\omega_1^2}{4} + \omega_0^2} + \frac{\omega_1}{2}$: the mode of p_A has a smaller threshold ϵ_1 for large ω_1 ($> 2\omega_0/\sqrt{3}$), and is thus more easily excited for large ω_1; the mode of p_B is more easily excited for small $\omega_1 < 2\omega_0/\sqrt{3}$ (see Fig. 13). Note that while this analysis is strictly valid only for sufficiently small ϵ_1 (e.g. $\epsilon_1/2 < \omega_0, \mu_1$), these are helpful in understanding non-monotonic response of our system to periodic modulation as shall be shown shortly. For the purpose of elucidating the effect of the modulation in α, we keep $\beta = 1$ in the following subsections.

A. Periodic self-amplification: $\alpha = \epsilon_1 \sin(\omega_1 t)$ and $\beta = 1$

In the presence of nonlinear damping term ($\beta \neq 0$), an exponentially growing solution saturates to finite amplitude, its solution forming a limit cycle for regular periodic oscillation, or strange (chaotic) attractor for irregular oscillation. To elucidate the effect of fluctuating α on nonlinear solution, we start with the case $\mu_1 = 0$ where $\alpha = \epsilon_1 \sin(\omega_1 t)$ is periodic and examine if this periodic modulation alone can excite finite amplitude solution. To this end, we compute solution to Eq. (1) numerically by keeping $\beta = 1$, for simplicity, and by varying ϵ_1 and ω_1. With no loss of generality, we are using the unit where $\omega_0 = 1$. After obtaining a long time trace of x and v, we compute phase-portrait and power-spectrum by taking Fourier transform of time trace after removing initial transients.

1. $\omega_1 = 2\omega_0$

As noted in Appendix A, when $\omega_1 = 2\omega_0 = 2$, a linear mode with frequency $p_A = \omega_1/2$ grows exponentially for all values of ϵ_1. Although the onset of linear instability is not necessarily the same as the onset of finite amplitude non-linear solution, in our case, we check by solving Eq. (1) for different values of ϵ_1 that finite amplitude nonlinear solution also exists for all values of ϵ_1. Specifically, a periodic limit cycle with frequency $\omega_1/2 = 1 = \omega_0$ is found up to $\epsilon_1 \sim 2.5$, which then gradually becomes more irregular with the development of sub-harmonics and then a chaotic attractor, interspersed by a periodic limit cycle via frequency locking for larger value of ϵ_1. Note that a similar behaviour was found for the Van der Pol oscillator [27] driven by an additive periodic forcing [38].

As an illustration, phase-portraits and frequency spectra are shown for $\epsilon_1 = 1$, 3, 3.6, 4.2, 5, and 6 in Fig. 1. Frequency spectrum with sharp peaks for $\epsilon_1 = 1$, 3.6, 4.2, 5 and 6 represents a limit cycle for a periodic oscillation, as can also be seen from a closed orbit in corresponding phase portrait. The smallest frequency of peaks in frequency spectrum is the angular frequency related to the mean period, which will be discussed shortly (e.g. Fig. 2). In comparison, continuous frequency spectrum and compact phase portrait for $\epsilon_1 = 3$ indicate irregular, chaotic oscillation. From the location of the peak at the smallest frequency and the shape of the frequency spectrum in Fig. 1, we can identify bifurcations such as the transition to chaos, frequency locking, sudden change in period (e.g. period doubling) as ϵ_1 increases. For instance, the leftward movement of the peak at the smallest frequency as $\epsilon_1 = 5$ increases to $\epsilon_1 = 6$ indicates the increase in period.

As mean period and variance are often used clinically (see also Appendix C) as diagnostics, we opt to utilise them to understand our results systematically. To this end, from the time trace of x, we determine the position of local maxima (peaks) of x where x takes its local maximum and compute the distance between two adjacent peaks (i.e. peak-peak distance) which is the time between two adjacent peaks. From this, we compute mean period and variance as a measure of mean peak-peak distance and its variation. Note that mean period is inversely related to mean frequency although a strict inverse relation does not hold as $\langle T \rangle = \langle 1/f \rangle \neq 1/\langle f \rangle$ where T and f are period and frequency, respectively while the angular brackets $\langle\rangle$ denote mean value. On the other hand, variance is linked to irregularity/complexity of oscillation, a small variance suggesting a regular periodic oscillation while a large variance suggesting an irregular, chaotic oscillation. We also measure maximum value and root-mean-square (rms) value of x.

Results are shown in Fig. 2(a) where mean period, variance, and maximum and rms value of x are plotted against ϵ_1 in blue, red, green and black. From Fig. 2(a), non-zero solution is seen to exist for all $\epsilon_1 \neq 0$, as noted previously. The period of the solution

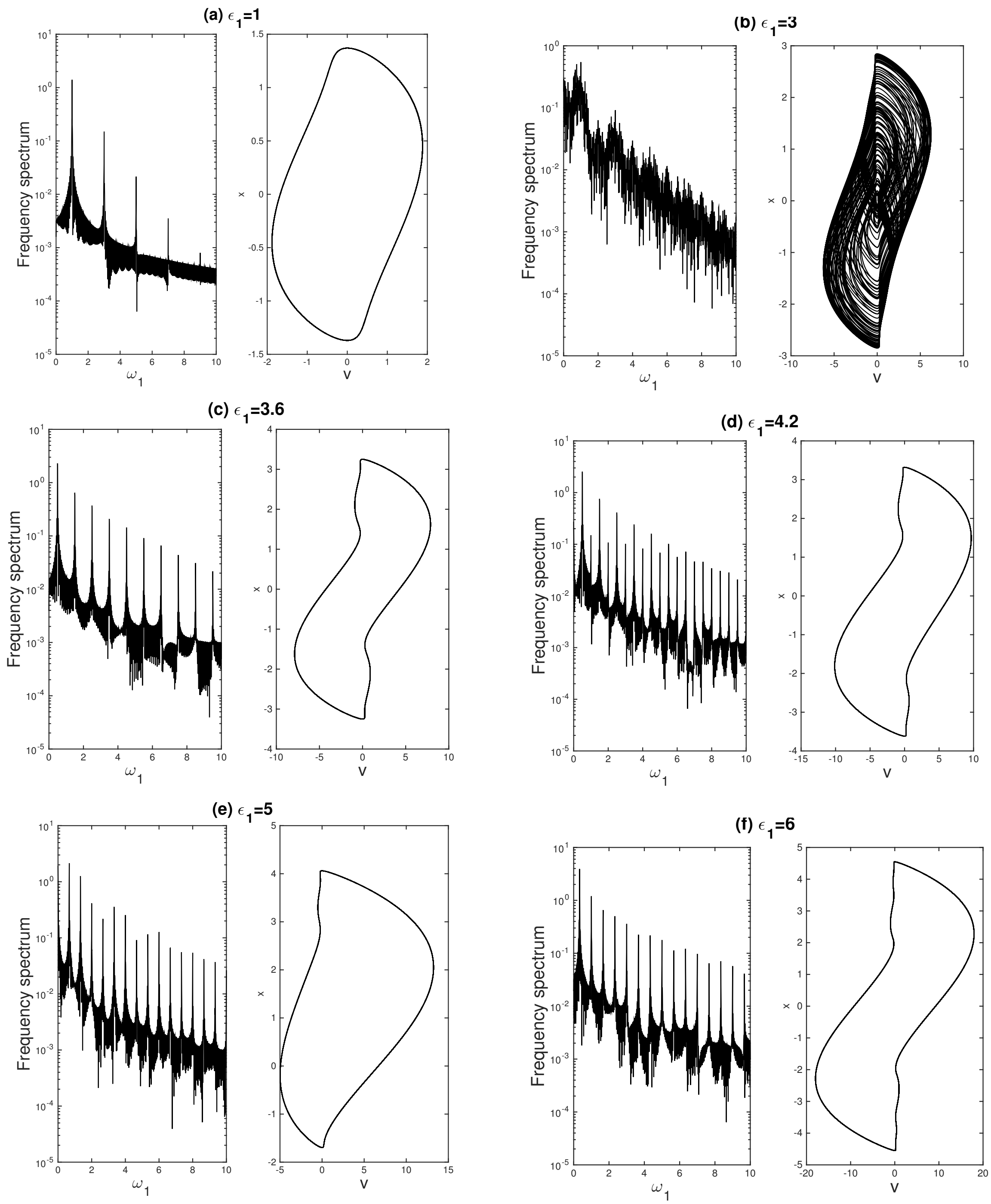

FIG. 1: Frequency spectrum of v against ω_1 and phase portrait in x-v plane for $\mu_1 = 0$, $\omega_1 = 2$, and $\beta = 1$.

(shown in blue) keeps its constant value $2\pi/\omega_0 = 2\pi$ up to $\epsilon_1 < 2.6$ then becomes almost double between $\epsilon_1 = 3.6$ and 4.2 where half frequency–mode $\omega_1/4 = \omega_0/2$ (period doubling) appears. Regular periodic oscillation for $\epsilon_1 < 2.6$ is indicated by a very small variance (plotted in red). The transition between two periodic limit cycles occurs through large

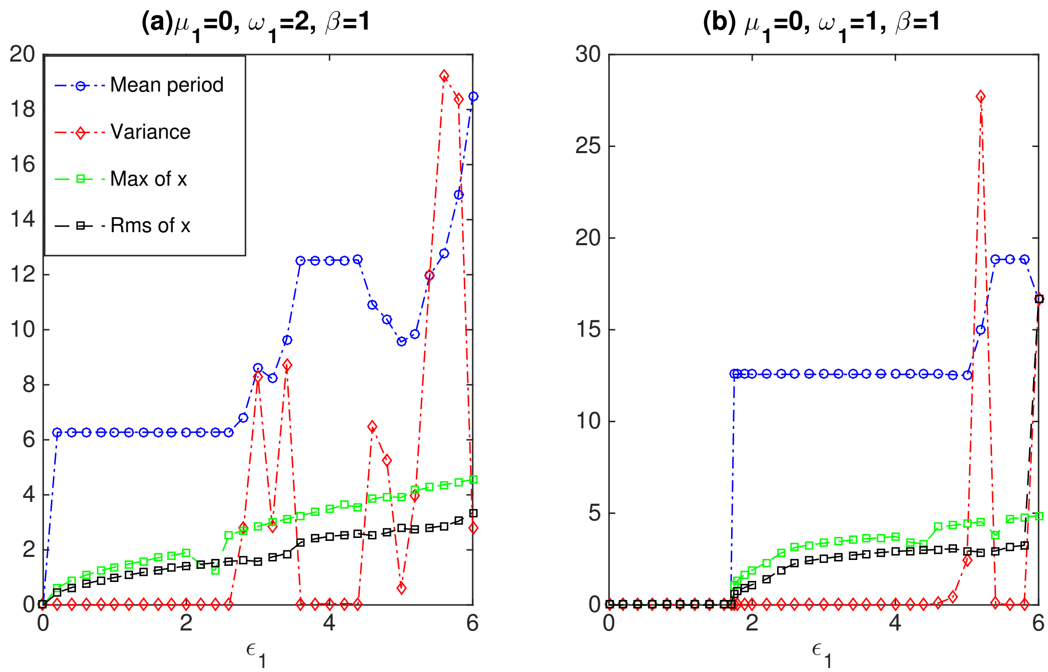

FIG. 2: Mean period (in blue), variance (in red), maximum (in green) and rms values (in black) of x against ϵ_1 when $\mu_1 = 0$ and $\beta = 1$.

variance, indicating the involvement of irregular oscillation such as chaos (e.g. as also shown in Fig. 1(b)), quasi-periodicity, etc. For $\epsilon_1 > 4.2$, oscillation tends to become yet more complex with larger variance together with increasing mean period although there appears a small region of regular oscillation with period three (through frequency locking at frequency $\omega_1/3 = 2\omega_0/3$ and $\omega_1/6 = \omega_0/3$ at $\epsilon_1 = 5$ and $\epsilon_1 = 6$, respectively [39]). See Fig. 1 for the corresponding frequency spectra and phase portraits. In comparison with mean period and variance, maximum (in green) and rms value of x (in black) exhibit much simpler, almost linear dependence on ω_1. Similar behaviour will also be seen later in the presence of non-zero μ_1 (see Fig. 4).

2. $\omega_1 = \omega_0$

Unlike the case of $\omega_1 = 2$, a linear solution for the modulation frequency $\omega_1 = 1$ requires a finite value of $\epsilon_1 \geq \sqrt{3}$ to grow exponentially. We first check that the onset of finite amplitude nonlinear solution requires the same critical value $\epsilon_1 = \sqrt{3}$. This is seen in Fig. 2(b) where damped solution for $\epsilon_1 < \sqrt{3}$ is indicated by zero values of mean period, variance,

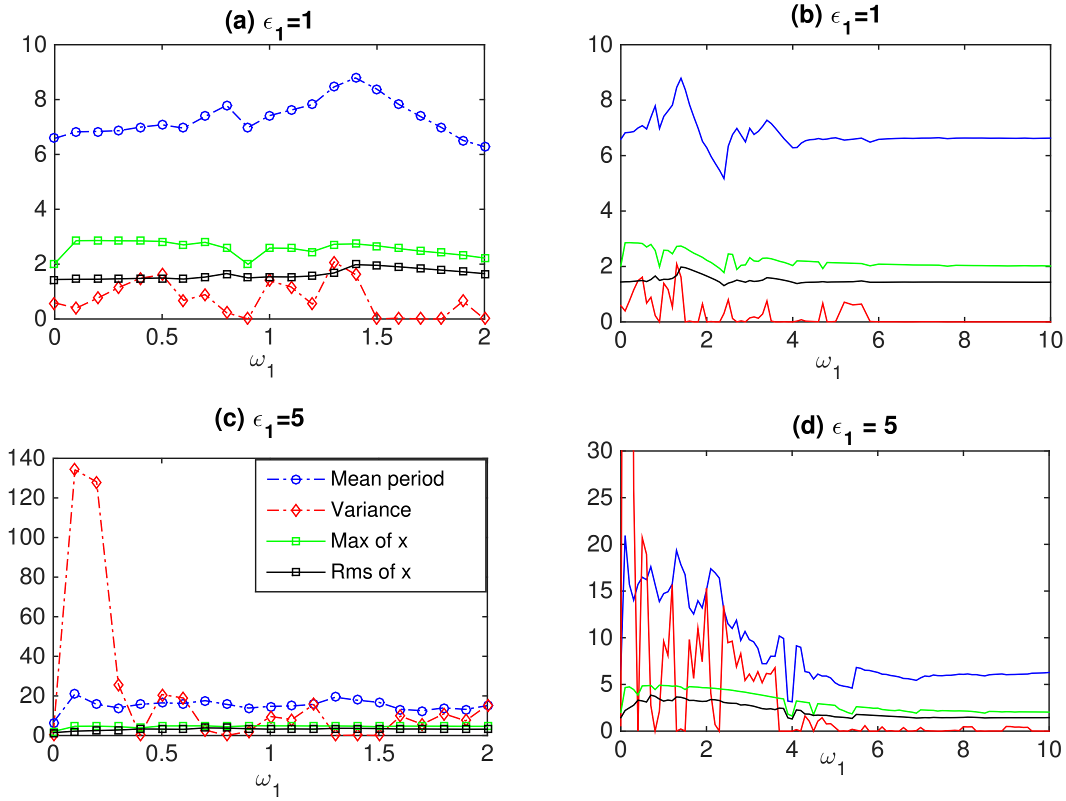

FIG. 3: Mean period (in blue), variance (in red), maximum (in green) and rms values (in black) of x against ω_1 when $\mu_1 = 1$ and $\beta = 1$; (a)-(b): $\epsilon_1 = 1$; (c)-(d) $\epsilon_1 = 5$.

and maximum and variance of x. At the onset of finite amplitude solution at $\epsilon_1 = \sqrt{3}$, nonlinear oscillation is periodic with frequency $\omega_1/2 = 0.5$ with negligible variance. The oscillator maintains this frequency for a long interval ϵ_1 up to $\epsilon_1 \sim 4.8$ and becomes chaotic for a short interval $4.8 \leq \epsilon_1 \leq 5.2$ before becoming periodic via frequency locking at $\omega_1/3$ (period three) when $\omega_1 \sim 5.4$. A noticeably large variance (shown as a big red spike) in the transition region is a symptomatic of chaos. In comparison, maximum (in green) and rms value of x (in black) again exhibit much simpler, almost monotonic increase with ω_1, as observed previously in Fig. 2(a).

B. $\alpha = 1 + \epsilon_1 \sin(\omega_1 t)$ and $\beta = 1$

A positive constant $\alpha = \mu_1 > 0$ in Eq. (2) leads to self-amplification of the Van der Pol oscillator. The addition of periodic modulation $\epsilon_1 \sin(\omega_1 t)$ to α in Eq. (2) thus further promotes the growth of the solution. In the following, we fix $\mu_1 = 1$ and $\beta = 1$ and present results for the three cases of different parameter scan over ϵ_1 and ω_1.

1. $\epsilon_1 = 1$

We start with the case when the amplitude ϵ_1 of the periodic modulation is comparable to the constant part $\mu_1 = 1$ in which case α varies between 0 and 2 in time, remaining non-negative for all time. Our results are shown in Fig. 3(a)-(b) by using the two different intervals of ω_1 on the x axis. For small ω_1, interesting non-monotonic behaviour of mean period and variance is pronounced. In particular, the variance becomes very small around $\omega_1 = 0.9$ where the frequency of solution becomes equal to the modulation frequency ω_1, indicated by a periodic limit cycle with the frequency $p = 0.9 = \omega_1$. Another noticeable periodic solution is observed over a finite range of $1.5 \leq \omega_1 \leq 1.8$ where the nonlinear oscillator has 3/2 period ($\sim$ 9), likely by frequency locking. In contrast, the maximum amplitude and rms value of x show much weaker dependence on ω_1 than mean period and variance. When ω_1 is sufficiently large (e.g. $\omega_1 > 5$), mean period, variance, maximum and rms value of x asymptotically approach the values in the absence of the periodic modulation $\epsilon_1 = 0$. This is because the effect of $\epsilon_1 \sin \omega_1 t$ vanishes as $\omega_1 \to \infty$ as a system cannot respond to too rapid perturbation/modulation in a parameter.

2. $\epsilon_1 = 5$

We now consider the case where the amplitude ϵ_1 of fluctuation in α is much larger than the constant part by choosing much larger $\epsilon_1 = 5$ and show results in Fig. 3(c)-(d). In comparison with Fig. 3(a)-(b), we observe that varying ω_1 between 0 and 1 has a much larger effect on the mean period and variance as the strength of perturbation is larger. Note that it is also possible that for this range of small ω_1, the second mode of frequency p_B plays an important role as this mode is more easily excitable at low frequency (see the discussion in §II and Appendix A). Variance is observed to be very small around $\omega_1 = 0.4, 0.8$ and 1.2 where the mean period takes approximately the same value 15.7. Interestingly, the corresponding frequency $2\pi/15.7 = 0.4$ exactly matches the frequency (ω_1), half frequency ($\omega_1/2$) and quarter frequency ($\omega_1/4$) for $\omega_1 = 0.4, 0.8$ and 1.2, respectively, indicative of nonlinear frequency locking. In comparison, the maximum and rms values of x vary much less, as in the case of $\epsilon_1 = 1$. For a sufficiently large ω_1 (greater than 5), the values remain constant upon the further increase in ω_1, due to the disappearance of the effect of periodic modulation for too large ω_1, as observed previously.

3. $\omega_1 = 1$

Finally, we now look at the effects of changing the amplitude ϵ_1 for a fixed $\omega_1 = 1$. Results in Fig. 4 show that a periodic solution with an almost constant output frequency is maintained over a rather long range of ϵ_1 where variance is negligibly small. Specifically, for $\epsilon_1 \leq 0.2$, mean period is about 6; for $0.3 \leq \epsilon_1 \leq 1$, it gradually increases; for $1.2 \leq \epsilon_1 < 1.8$, it fluctuates around 8.3 (with the dominant frequency 0.75); for $2.2 \leq \omega_1 \leq 3.2$, the period becomes 12.57, which is half a modulation frequency $\omega_1/2$ (i.e. period doubling). Period three 18.985 at the third of modulation frequency $\omega_1/3$ is also noticeable for a short interval $5.2 \leq \epsilon_1 \leq 5.4$. The transition between two nearby periodic limit cycles is accompanied by bifurcation involving chaotic oscillation, quasi-periodicity, etc with large variance. In contrast, maximum and rms value change smoothly upon the change in ϵ_1, increasing almost linearly with increasing ϵ_1, as also observed in Fig. 2.

It is instructive to compare Fig. 4 with Fig. 2(b) obtained for the same parameter values apart from μ_1. The most notable difference between these two figures is the existence of finite amplitude solution for all value of ϵ_1 in the case of $\mu_1 = 1$ in Fig. 4, while non-zero solution exists only for $\epsilon_1 > \sqrt{3}$ in Fig. 2(b). This is because μ_1 excites oscillation even when $\epsilon_1 = 0$. Another difference is that the period doubling occurs at a larger value of ϵ_1 in Fig. 4 compared to that in Fig. 2(b), which is again due to the effect of μ_1. For large ϵ_1 (> 2.2), Fig. 4 and Fig. 2(b) exhibit quite similar tendency.

IV. FLUCTUATION IN NEGATIVE FEEDBACK: $\alpha = 1$, $\beta = 1 + \epsilon_2 \sin(\omega_1 t)$

Self-regulation of the Van der Pol oscillator is modelled by a cubic nonlinear damping term with a positive constant β. In order to understand how self-regulation is affected by fluctuation, we consider $\beta = \mu_2 + \epsilon_2 \sin(\omega_1 t)$ as given in Eq. (3) while we fix $\mu_2 = 1$ and $\alpha = 1$, for simplicity, and explore the possibility of the breakdown of self-regulation.

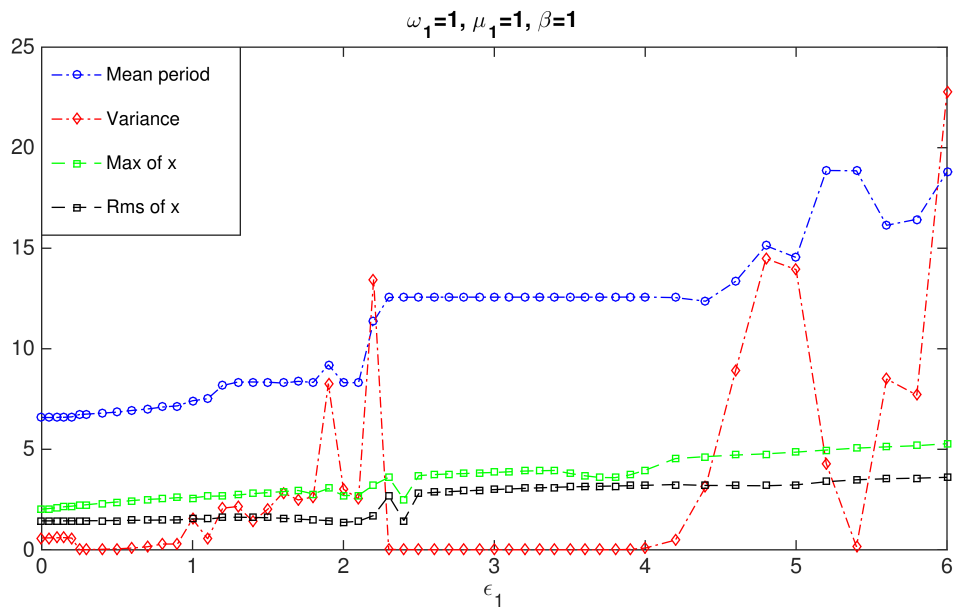

FIG. 4: Mean period (in blue), variance (in red), maximum (in green) and rms values (in black) of x against ϵ_1. Parameters are $\omega_1 = 1$, $\mu_1 = 1$, $\beta = 1$.

A. $\omega_1 = 1$

Results are shown in Fig. 5 for $\omega_1 = 1$ and $\epsilon_2 \leq 1$. It is apparent that as ϵ_2 increases from zero, mean period increases marginally, followed by a sudden increase between $\epsilon_2 = 0.7$ and $\epsilon_2 = 0.8$ where it is doubled from 2π to 4π. Between these points, the transition involves large variance due to irregular oscillation. In comparison, maximum amplitude and rms value of x increase steadily for increasing ϵ_2, with the tendency of faster increase as $\epsilon_2 \to 1$. The maximum value of ϵ_2 shown in Fig. 5 is 1 since for a larger value of $\epsilon_1 > 1$, a solution grows exponentially due to inefficient negative feedback. This is elaborated in the next subsection.

B. Breakdown of self-regulation: Critical regulation point

To help understanding the effect of ϵ_2 on self-regulation, $\beta = \mu_2 + \epsilon_2 \sin(\omega_1 t)$ is shown in Fig. 6 for $\epsilon_2 = 0.5$ and $\epsilon_2 = 1.5$ by using the fixed value of $\mu_2 = 1 = \omega_1$. It is clear that when $\epsilon_2 \leq \mu_2$, β is positive for all t, preventing a linear solution from growing exponentially. However, when $\epsilon_2 > \mu_2$, β takes negative values for certain time interval during which

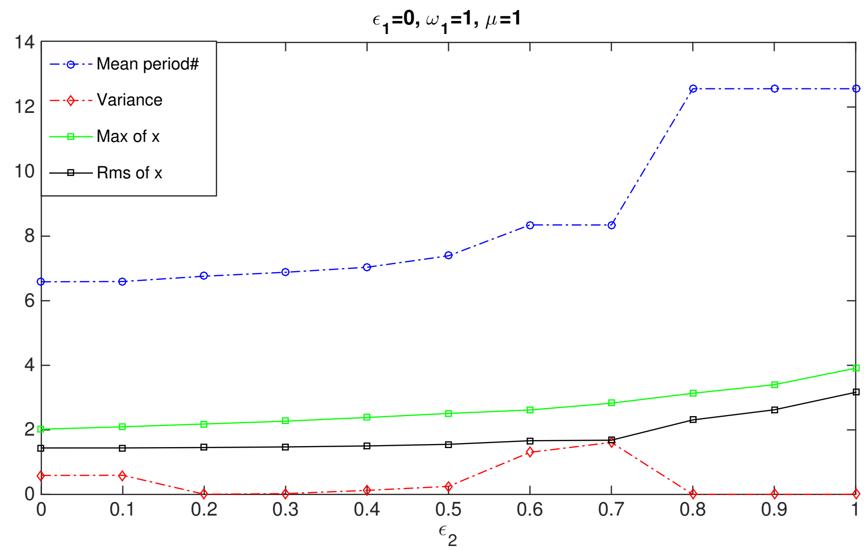

FIG. 5: Mean period (in blue), variance (in red), maximum (in green) and rms values (in black) of x against ϵ_2. Parameters are $\epsilon_1 = 0$, $\omega_1 = 1$, $\mu = 1$

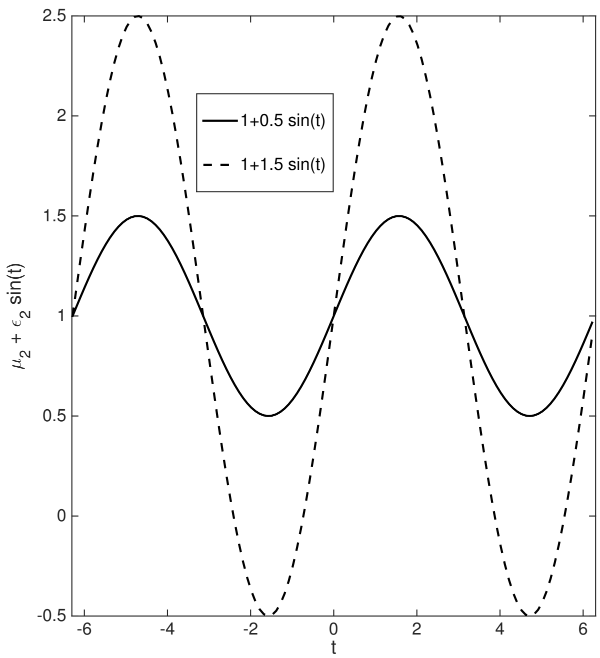

FIG. 6: The effect of fluctuating β.

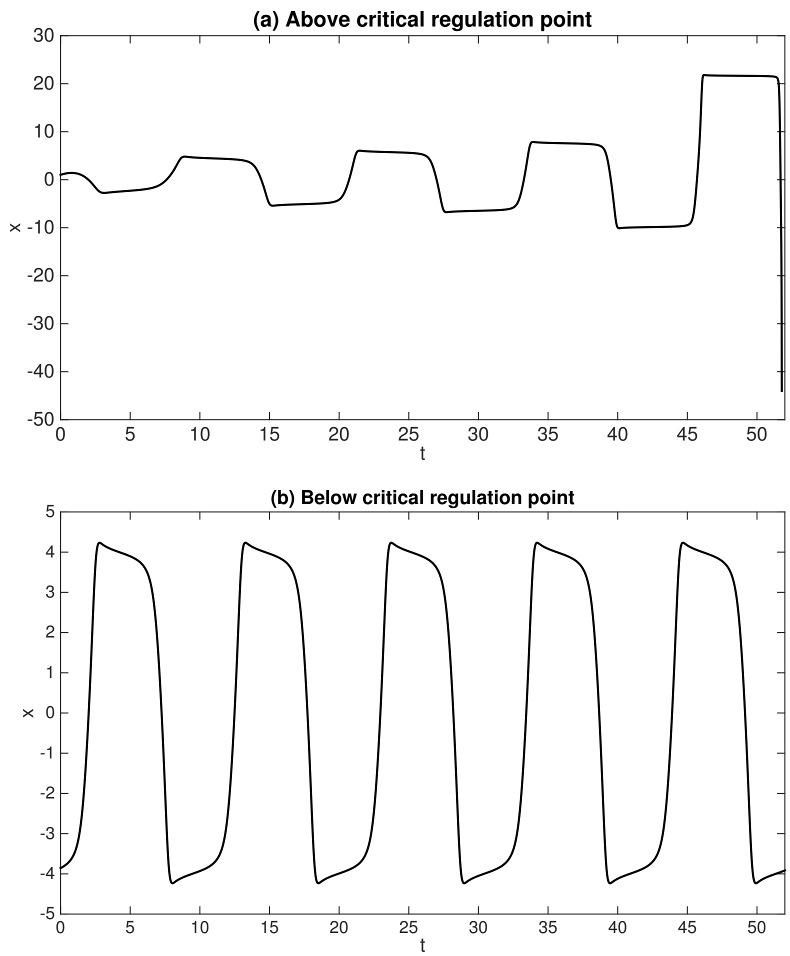

FIG. 7: Comparison between the two cases of (a) $\omega_1 = 1$ (below critical value) and (b) $\omega_1 = 1.2$ (above critical value) for the fixed parameter values $\epsilon_2 = 1.1$ and $\alpha = \mu_2 = 1$.

the solution can grow exponentially. Therefore, when $\epsilon_2 > \mu_2$, there are intervals of time when the solution exponentially grows, sandwiched between time intervals when the solution damps. The overall effect of this alternative growth and damping of the solution depends on the value of ω_1 for fixed ϵ_2 since the smaller ω_1, there is a longer time for a solution to grow to substantial amplitude before it gets damped. In comparison, larger ω_1 allows less time for the solution to grow so that the amplitude of the solution can be regulated to finite value. In the extreme limit of $\omega_1 \to \infty$, the effect of periodic oscillation disappears as observed previously, with $\beta \to \mu_2 > 0$. Thus for a given $\epsilon_2 > \mu_2$, there exists the minimum ω_1, corresponding to a critical value of ω_1 below which self-regulation is lost and the solution grows exponentially. This critical point is referred as a regulation point.

One example of this is shown in Fig. 7(a) for $\epsilon_2 = 1.1$ and $\omega_1 = 1$ (below critical value) and Fig. 7(b) for $\omega_1 = 1.2$ (above critical value). For $\omega_1 = 1$ (below critical value), a limit cycle exhibits a few oscillations before succumbing to the exponential growth. This is because ω_1 is not quite large enough, permitting a sufficiently long time for the solution to grow exponentially in Fig. 7(a). As ω_1 is slightly increased to $\omega_1 = 1.2$ in Fig. 7(b), there is less time for a solution to grow exponentially, making regulation possible.

ϵ_2	1.01	1.1	1.3	1.5	1.6	1.65	1.7	1.8	2	3	5	10	20	50	100	200
ω_1	0.4	1.2	1.9	2.4	2.6	2.7	5.5	5.9	6.6	9.4	13	19.2	29.5	58	98.3	163
Mean period	31.5	10.4	6.5	5.2	4.8	4.8	4.6	5.0	5.5	4.8	4.5	3.6	3.0	2.2	1.5	1.0

TABLE I: Relation between ϵ_2 and ω_1 for critical point for $\mu_1 = 1$ and $\epsilon_1 = 0$.

To find the relationship between ϵ_2 and ω_1 for a regulation point, it is simply a case of choosing some $\epsilon_2 > \mu_2$ and finding the minimum ω_1 such that the output is regulated with a finite amplitude solution. The regulation points that we find are tabulated in Table. I. We observe that as ϵ_2 increases, ω_1 increases. Note that the mean period markedly decreases for increasing ϵ_2 (this will be utilised in §V.B).

V. IMPLICATIONS FOR HEART DYNAMICS

Results shown in previous sections demonstrated a significant change to the Van der Pol oscillator due to periodic modulation in model parameters, highlighting an important role of fluctuations in positive and negative feedback. In this section, we explore some of implications of these results for heart dynamics as an example. It is useful to note that applied to heart model, the distance between two adjacent peaks (peak-peak distance) of x could be interpreted as peak-peak distance in action potential (see Fig. 14 and more discussion in Appendix B) or the time between two adjacent heart beats. Thus, the inverse of mean period represent average heart rate while the variance in peak-peak interval is related to heart rate variability [29–31] (see Appendix C for implication for heart variability).

A. Incoherent positive feedback

We recall that α represents the efficiency of positive feedback and takes a constant value when this positive feedback is coherent while the decrease in efficiency is modelled by fluctuations in α. In the case of heart, α could be viewed as the contribution to action potential from ion currents across membrane, which change electric potential (e.g. depolarisation) at cellular level, or as the effect of the conduction of electric potential through cardiac tissues from Sinus node to Perkinjee fibre at tissue level. Even though fluctuating α is less efficient than constant α, we observed in Section III.A that a purely periodic α permits self-excitation of oscillation as long as the frequency (the amplitude) of α is not too large (too small). This suggests that fluctuating ion currents can initiate early depolarisation of action potential.

Another important implication would be for modelling abnormal heart rhythm associated with slow heart (heart block or heart failure). There are different ways that lead to heart failure (e.g. see [28, 32–34] and references therein). One way would be via amplitude death where oscillation amplitude gradually decreases until it goes away (e.g. through Hopf bifurcation); another would be via increased period associated with skipped beats (e.g. through Homoclinic bifurcation). As an illustration, we here show a few examples of how the results in Section III.A-III.B can be utilised to model these two pathways.

1. *Amplitude death*

Based on the results in Section III.A, we propose that one possible pathway of amplitude death is by the progression of incoherent positive feedback and model this by time dependent $\alpha(t)$ as

$$\alpha(t) = \mu_1(t) + \epsilon_1(t)\sin(\omega_1 t),\ \ \mu_1(t) = \mu_0(1 - F(t)),\ \ \epsilon_1(t) = \epsilon_0 F(t), \tag{4}$$

where μ_0 and ϵ_0 are constant while $F(t)$ is time-dependent function. As the efficiency of positive feedback degrades in time, fluctuation ϵ_1 will increase due to incoherent positive feedback at the loss of the constant μ_1. Thus, we take $F(t)$ to be a monotonically increasing function of time, taking the value between 0 and 1, so that the constant part of $\mu_1(t)$ decreases from μ_0 to 0 while the oscillatory part of $\mu_1(t)$ increases from 0 to μ_0 in time. As an example, we choose $F(t) = \tanh(t/\tau)$ where τ is the characteristic time scale of $F(t)$ and show results for $\tau = 100$, $\mu_0 = \epsilon_0 = 1$, $\omega_1 = 1$ and $\beta = 1$ in Fig. 8. In Fig. 8(a),

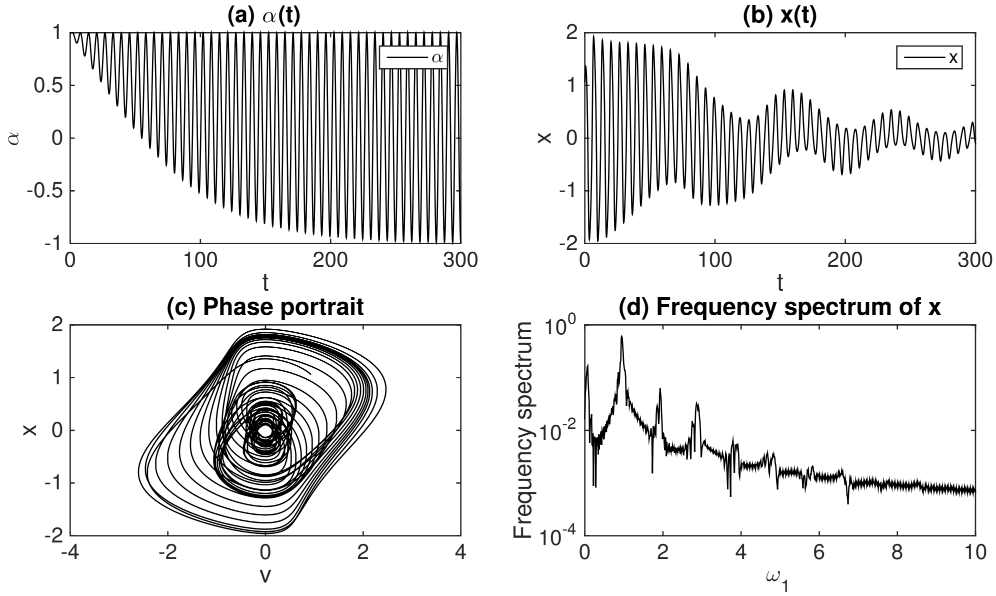

FIG. 8: $\alpha(t) = \mu_0(1 - F(t)) + \epsilon_0 F(t) \sin(\omega_1 t)$ and $\beta = 1$ with $F(t) = \tanh(t/100), \mu_0 = 1, \epsilon_0 = 1, \omega_1 = 1$.

$\alpha(t)$ starting from constant value 1 is seen to increase its fluctuation with t according to Eq. (4), while keeping its maximum value 1. The plot of v against t in Fig. 8(b) as well as the phase portrait in Fig. 8(c) clearly show how the oscillation amplitude decreases with time as a result. The corresponding frequency spectrum shown in Fig. 8(d) reveals well-defined peaks, indicating the persistence of the oscillation with almost the same frequency, regardless decreasing oscillation amplitude.

2. Oscillation death

The key observation we can make from Figs. 3-4 is that mean period depends most sensitively on the amplitude of fluctuation ϵ_1 with the interesting tendency of larger period for larger ϵ_1. To utilise this, we choose the value of $\epsilon_1 = 6$ by keeping all other parameter values the same as in Fig. 8 and show the results in Fig. 9. In Fig. 9(a), α starting from the constant value 1 increases its fluctuations, taking the value between -6 and 6 (with zero time average value at a sufficiently large time). From the time history of x in Fig. 9(b), we observe that the oscillation changes its period (the interval between two peaks) around $t \sim 140$ where the period suddenly increases accompanied by a missed oscillation. The phase

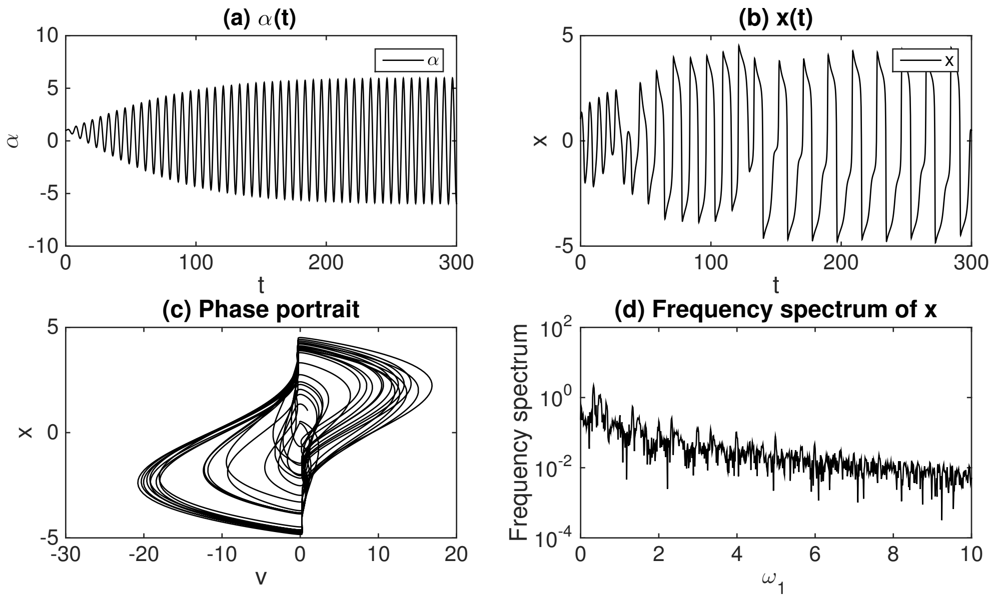

FIG. 9: $\alpha(t) = \mu_0(1 - F(t)) + \epsilon_0 F(t) \sin(\omega_1 t)$ and $\beta = 1$ with $F(t) = \tanh(t/100), \mu_0 = 1, \epsilon_0 = 6, \omega_1 = 1$.

portrait in Fig. 9(c) and the frequency spectrum in Fig. 9(d) reveal the presence of different frequencies due to this change. These results clearly show how a pathway to an oscillation death via missed peaks proceeds in time.

To demonstrate the robustness of our results, we show two more cases by using $\mu_0 = 1$ and $\epsilon_0 = 12$ and $\mu_0 = 6$ and $\epsilon_0 = 6$ in Fig. 10 and Fig. 11, respectively, where similar behaviour can be observed. It is quite entertaining to see how the decrease in oscillation frequency proceeds in Figs. 10(b) and 11(b). Of particular intrigue in Fig. 11 is that period doubling occurs even when the constant part of α before the transition is comparable to the amplitude of fluctuating part after the transition.

Finally, it is important to note that the fact that the only difference between Figs. 8 and 9, representing amplitude death and oscillation death pathways, respectively, is the strength of fluctuations alludes to the possibility that amplitude and oscillation death may have the same origin of incoherent positive feedback; that is, amplitude death is a consequence of small fluctuation in positive feedback while oscillation death is a consequence of large fluctuation in positive feedback.

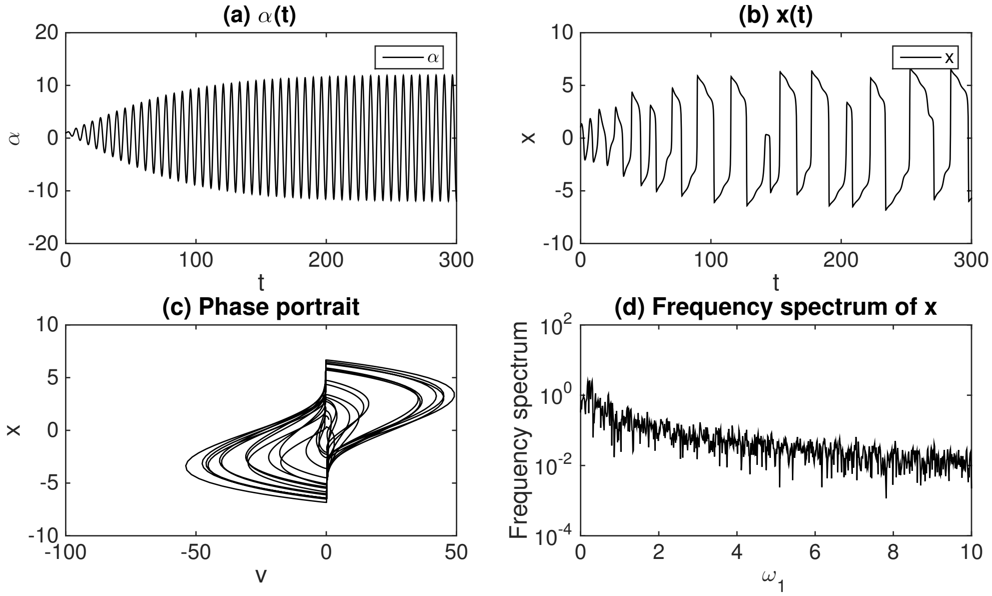

FIG. 10: $\alpha(t) = \mu_0(1 - F(t)) + \epsilon_0 F(t)\sin(\omega_1 t)$ and $\beta = 1$ with $F(t) = \tanh(t/100), \mu_0 = 1, \epsilon_0 = 12, \omega_1 = 1$.

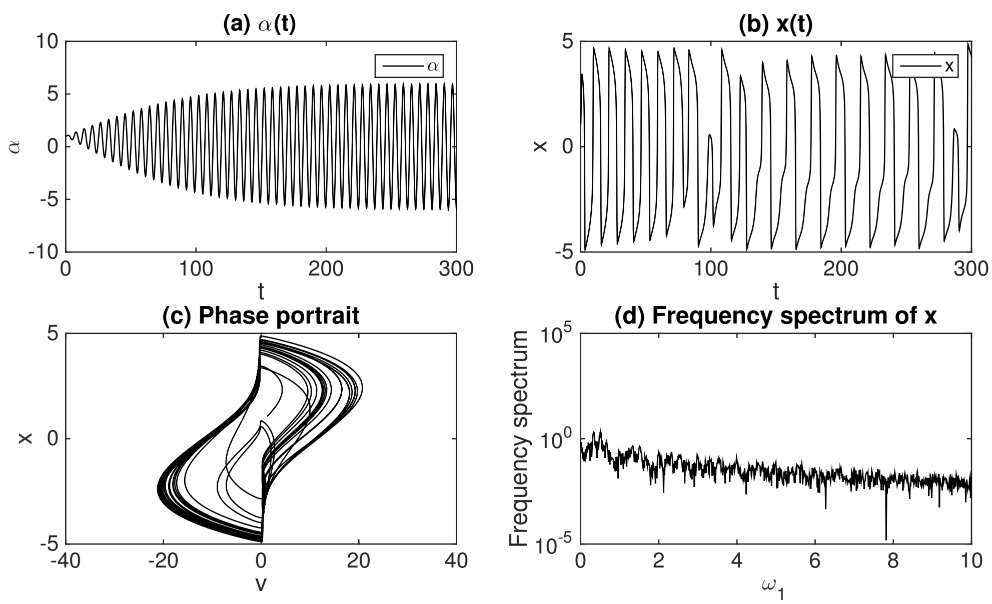

FIG. 11: $\alpha(t) = \mu_0(1 - F(t)) + \epsilon_0 F(t)\sin(\omega_1 t)$ and $\beta = 1$ with $F(t) = \tanh(t/100), \mu_0 = \epsilon_0 = 6, \omega_1 = 1$.

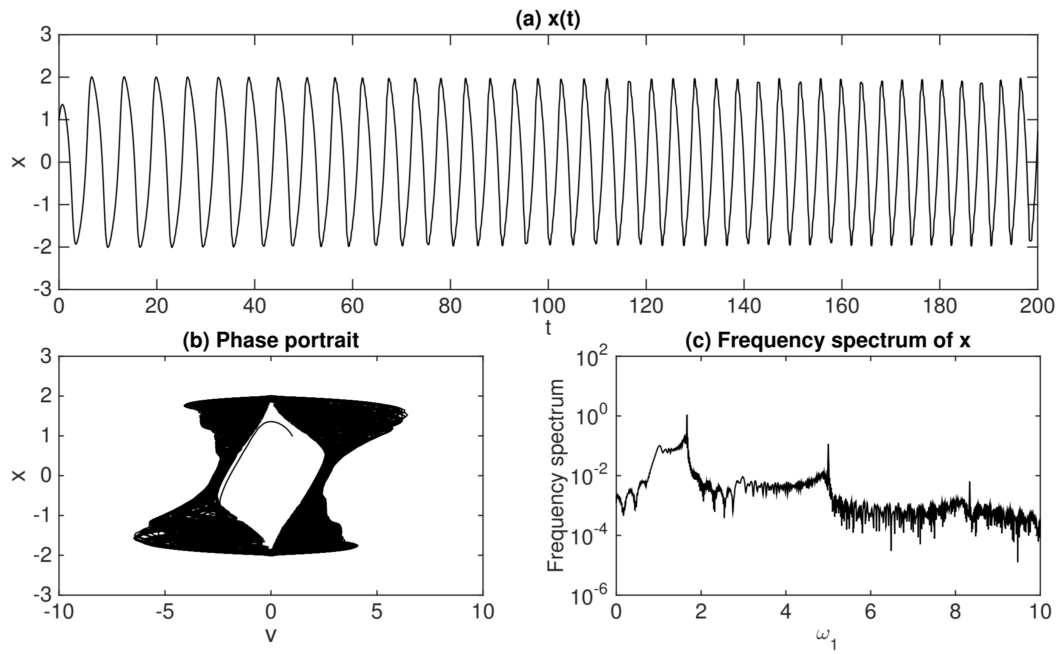

FIG. 12: $\alpha = 1$, $\beta = 1 + \epsilon_0 \sin(\omega_1 t) \tanh(t/100)$ with $\epsilon_0 = 10$ and $\omega_1 = 20$.

B. Incoherent negative feedback

As seen in Section IV, near the regulation point, mean period tends to decrease for larger fluctuation ϵ_2 in β (see Table 1). We now show how these results could be utilised to model a progression to fast heart rhythm (e.g. tachycardia). We model the increase in fluctuation in β by taking the following time-dependent function:

$$\beta(t) = \mu_2 + \epsilon_0 \sin(\omega_1 t) \tanh(t/100), \tag{5}$$

and results obtained for $\mu_2 = 1$, $\epsilon_0 = 10$, and $\omega_1 = 20$ are plotted in Fig. 12. Fig. 12(a) clearly shows that the period of oscillation becomes shorter in time when the fluctuating β increases according to Eq. (5); phase portrait and frequency spectrum in Figs. 12(b) and 12(c) reveal the involvement of a mixture of different frequencies of oscillations in this processes.

VI. DISCUSSION AND CONCLUSION

While the variability has emerged as a key factor in sustainability, too much variability however could be detrimental. Our work was motivated to understand how homeostasis manifested in the form of self-sustained oscillations is affected by fluctuating parameter, modelled by periodic modulation. In particular, we were interested in identifying sweet-spot in variability in model parameter and the limits beyond which self-regulation breaks down. To this end, we focused on the effect of fluctuation in self-amplifying parameter (positive feedback) and nonlinear damping parameter (negative feedback) in the Van der Pol oscillator. Our general conclusions are summarised as follows:

- Self-sustained oscillation can be excited by a purely oscillatory self-amplifying parameter as long as its time rate of change is not too fast. This highlight the importance of fluctuations in positive feedback loop, e.g. such as fluctuating ion currents.
- Model parameter that changes too rapidly for a system to respond induces no change in the system. This is related to 'refractory (or recovery) time' required for an organism to be ready for a new stimulant, for example.
- Mean period and variance vary non-monotonically with fluctuation amplitude of model parameters while maximum and rms values tend to monotonically increase.
- The increase in fluctuation in positive feedback leads to the transition between the two periodic limit cycles by passing through a small region of chaos and/or quasi-periodicity, with the lengthening of oscillation period.
- A sudden change in oscillation period occurs via nonlinear frequency locking, which has been found in the previous work of pacemaker by a more complicated model (see, e.g. [28]).
- Periodic oscillation occurs within the bounds on variability in model parameter, beyond which a system could lose its sustainability. For instance, a long plateau region between $\epsilon_1 = 2.6$ and 4 in Fig. 4 may represent the bounds within which a self-sustained oscillator operates (i.e. sweet spot).

- Fluctuations in nonlinear damping make negative feedback less effective, leading to a possible overgrowth of the solution. This has interesting applications, such as tumour progression due to the incoherent self-regulation [12].

- Self-organisation can break down completely when negative feedback/regulation becomes inefficient due to incoherent nonlinear damping, with an exponentially growing solution. For the critical point for this breakdown, we noted an approximate linear relation between ϵ_2 and ω_1 (see §IV.B).

- Applied to heart dynamics, i) incoherent positive feedback can lead to slow heart by either amplitude death (§V.A.1) or oscillation death pathway (§V.A.2) when the fluctuation in α is sufficiently small or large, respectively; (ii) incoherent negative feedback can lead to fast heart beat (§V.B) [The importance of amplitude of fluctuation in feedback is further elaborated in Appendix C for heart rate variability.]

We recognise that there has been a great advancement in heart modelling, involving multi-scale, multi-disciplinary synergistic approach (e.g. see [28] and reference therein), and our intention was nowhere near such an attempt. Our purpose was instead to elucidate a key role of fluctuations in feedback loop and its consequence, which would not be feasible in a more complicated model. Despite its simplicity, our model has the merit of enabling us to undertake a systematic investigation, and, we hope, would prove to be a useful model to understand other self-regulation systems. It would be worthwhile to tailor and extend our work, for example, by i) investigating the effect of modulation of α and β with different frequencies, ii) incorporating the effect of stochastic fluctuation, iii) exploring the combined effect of multiplicative and additive noises, iv) considering more than two feedback loops, and v) including evolution equation for α and/or β.

We thank Drs L. Robson and M. Cambray-Deakin for their inspiration for the work. We also thank M Mohamed for her help with Matlab.

Appendix A: Linear dispersion relation

In this appendix, we provide a linear analysis on the effect of periodic damping. For simplicity, we take a Laplace transform of Eq. (1) to obtain

$$(\omega_0^2+\mu s+s^2)\tilde{x}(s)+\frac{\epsilon_1}{2i}\left[(s-i\omega_1)\tilde{x}(s-i\omega_1)-(s+i\omega_1)\tilde{x}(s+i\omega_1)\right]=\dot{x}(0)+(s+\mu)x(0), \quad (6)$$

where $\dot{x}(0)=\frac{dx}{dt}$ at $t=0$, $\tilde{x}(s)=\int_0^\infty dte^{-st}x(t)$. While Eq. (6) establishes an initial value problem, we are interested in the condition which gives rise to the (parametric) instability via frequency matching (i.e. resonance). To find this, we consider the dispersion relation by keeping the nearest interaction between the two adjacent modes $\tilde{x}(s)$ and $\tilde{x}(s-i\omega_1)$ as

$$(\omega_0^2+s^2+\mu s)\left[\omega_0^2+(s+i\omega_1)^2+\mu(s+i\omega_1)\right]-\frac{\epsilon_1^2}{4}s(s+i\omega_1)=0. \quad (7)$$

By taking $s=\gamma+ip$ where γ and p are real constants for the growth rate and frequency, we obtain from Eq. (7) the following two relations:

$$0 = (2p-\omega_1)\left[(2\gamma+\mu)[\omega_0^2+\gamma(\gamma+\mu)-p(p-\omega_1)]-\epsilon_1^2\gamma/4\right], \quad (8)$$

$$\begin{aligned}0 = {} & [\omega_0^2+\gamma(\gamma+\mu)-p^2][\omega_0^2+\gamma(\gamma+\mu)-(p-\omega_1)^2] \\ & -p(p-\omega_1)(2\gamma+\mu)^2-\frac{\epsilon_1^2}{4}[\gamma^2-p(p-\omega_1)]. \quad (9)\end{aligned}$$

The solutions to Eq. (8) are

$$p_A=\frac{\omega_1}{2},\ p_B=\sqrt{\frac{\omega_1^2}{4}+\omega_0^2}+\frac{\omega_1}{2}. \quad (10)$$

Using Eq. (10) in Eq. (9) establishes how the linear growth rate γ depends on the amplitude of the periodic perturbation ϵ_1. For instance, the onset of instability is obtained by putting $\gamma=0$ in Eq. (9), which gives us the critical value of ϵ_1 for the two modes as follows:

$$\epsilon_{1A} = \sqrt{4\mu^2+\frac{((2\omega_0)^2-\omega_1^2)^2}{\omega_1^2}}, \quad (11)$$

$$\epsilon_{1B} = 2\sqrt{\mu^2+\omega_1^2}. \quad (12)$$

The mode with frequency $p_A=\omega_1/2$ takes its minimum critical value $\epsilon_{1A}=2\mu$ when the modulation frequency $\omega_1=2\omega_0$, the twice natural oscillation frequency ω_0. This is due to the parametric resonance between the natural oscillation and periodic parameter, which facilitates resonant excitation of the mode with $\omega_1/2=\omega_0$. That is, the periodic

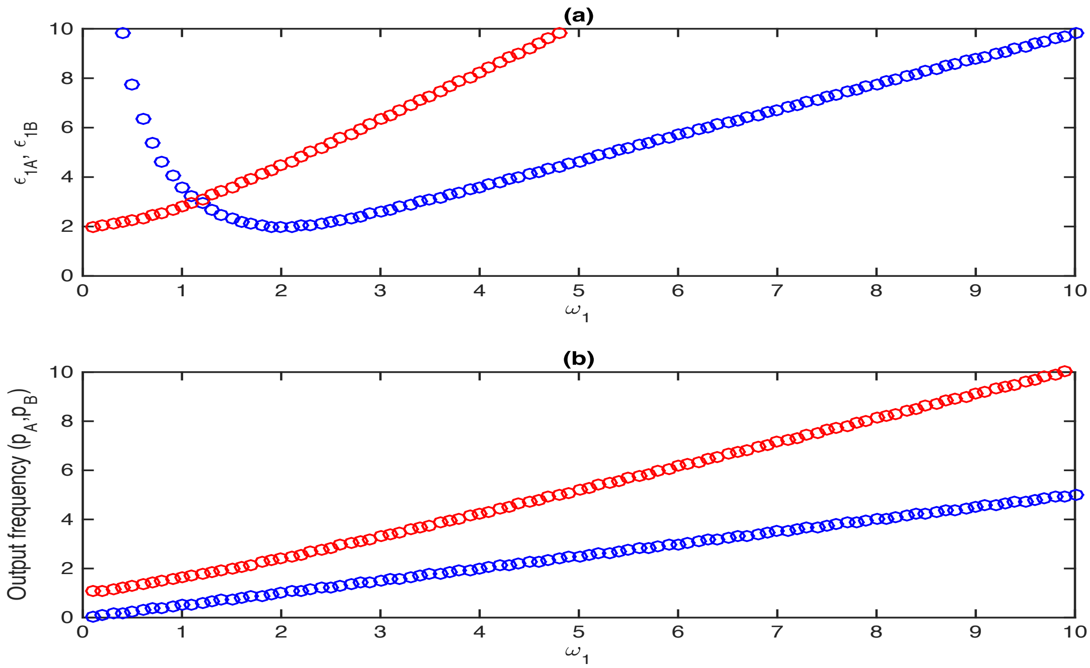

FIG. 13: Dispersion relation for the onset of instability when $\omega_0 = 1$, $\beta = 0$, $\mu_1 = 1$: (a) Critical ϵ_1 against input frequency ω_1; (b) Output frequency p against input frequency ω_1; (c) The product of input frequency and critical ϵ_1 against input frequency. Blue and Red lines are for the two solutions $p_A = \omega_1/2$ and $p_B = \sqrt{\omega_1^2/4 + \omega_0^2} + \omega_1/2$, respectively

parameter with twice natural frequency leads to the excitation of the mode, which has the same frequency as the natural frequency. This critical value $\epsilon_{1A} = 0$ when $\mu = 0$, implying the instability of the mode with frequency $p_A = \omega_1/2$ for all values of ϵ_1 and this mode dominates over the other mode with frequency p_B which requires a finite value $\epsilon_{1B} \geq 2\omega_1$ for excitation. We note that for finite μ, the critical value ϵ_{1A} for the mode with frequency $p_A = \omega_1/2$ is smaller than the mode with the frequency p_B for $\omega_1 > 2\omega_0/\sqrt{3}$ and is thus a dominant mode for sufficiently large ω_1. The opposite holds for small $\omega_1 < 2\omega_0/\sqrt{3}$ where the critical value ϵ_{1A} is smaller for the second mode with frequency p_B.

The critical values for these two modes are shown in blue and red lines in Fig. 13 by using $\omega_0 = \mu_1 = 1$ where the crossing between the two modes is seen at $\omega_1 = 2/\sqrt{3}$. The smallest critical value of ϵ_{1A} is clearly seen to occur at $\omega_1 = 2\omega_0$.

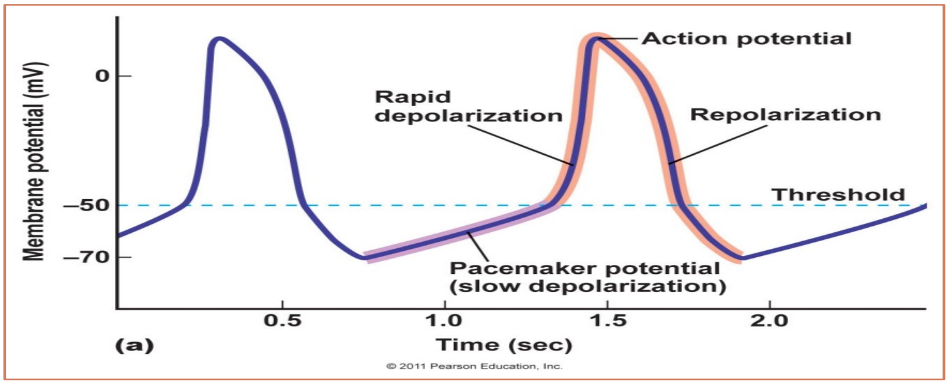

FIG. 14: Cardiac Action Potential

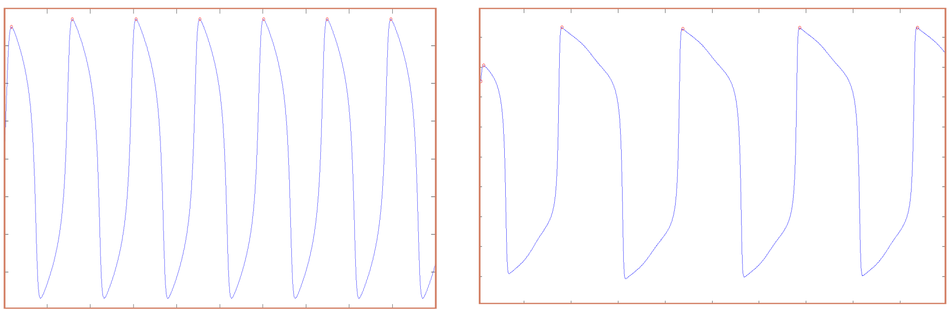

FIG. 15: (a) $\mu_1 = \mu_2 = 1.2, \epsilon_1 = \epsilon_2 = 0$; (b) $\mu_1 = \mu_2 = 1.2, \omega_1 = 1, \epsilon_1 = 1, \epsilon_2 = 0$.

Appendix B. Cardiac pacemaker

The main cardiac pacemaker periodically produces electric pulses to provide action potentials to the heart for relaxations and oscillations. A distinct feature of a cardiac pacemaker shown in Fig. 14 is a slow build-up followed by a sudden rise to a peak, which are known as pacemaker potential and rapid depolarization respectively. In the following, we show in detail that fluctuating parameters also have an important effect on the shape of the action potential as well as on the period.

To this end, we use parameter values $\mu_1 = \mu_2 = 1.2, \epsilon_1 = \epsilon_2 = 0$ and show the results in Fig. 15(a). Comparing Fig. 15(a) with Fig. 14, we see that the shape of the two is roughly similar. There is however much room for improvement, in particular, in the slow build-up of early depolarising phase and the overall shape of subsequent rapid and repolarisation phases. Specifically, the duration of the pacemaker potential in Fig. 15(a) is rather short compared to that seen in Fig. 14 while the overall shape of the action potential is rather smoother in Fig. 15(a) in comparison with Fig. 14. When we introduce the time-dependent model parameters as $\epsilon_1 = 1, \omega_1 = 1$ ($\epsilon_2 = 0$), we are able to make an improvement on this as shown in Fig. 15(b): the early depolarising phase appears to more resemble that of Fig. 14 with the relative duration of time for the build-up increasing. The action potential is also less steep, as hoped for. Although our model is not perfect, this is an improvement on the previous model, suggesting that a simply introducing time-dependent variables even by relatively small values can dramatically alter the model prediction.

Appendix C. Heart rate variability

The peak-peak distance in action potential (e.g. shown in Fig. 13) and the time between two heart beats can be inferred from the distance between the adjacent peaks (peak-peak distance) of x in our model. Therefore, the inverse of mean period quantifies the average heart rate while the variance in peak-peak interval is related to heart rate variability [29–31]. In human heart of healthy individual, heart rate is never constant but exhibits certain degree of variation as human heart is subject to many different factors ranging from rather regular to very irregular stimulants/input (e.g. modulation by breathing, input from nervous systems, etc). Application of the Van der Pol oscillator to heart dynamics thus requires the allowance of fluctuation in the model parameter to incorporate the effects from the variability. Also, as noted in the Introduction, as a model for oscillations in a continuous system in space such as heart, the Van der Pol oscillator is a mean-field theory, describing a large-scale, observable where fluctuating model parameter can capture spatial as well as temporal inhomogeneity (heterogeneity) in electro-chemical-mechanical activity (e.g. ion channel dynamics, electric conduction, muscle physiology, etc) contributing to heart dynamics. In fact, variability in heart rate has been known to be crucial for healthy heart, and there has been accumulating evidence that the decrease in variability is often associated with heart failure. On the other hand, too much variability in the form of tachycardia, etc, also leads to heart failure [29–34]. One of the interesting observation has been that the time between the two adjacent heart beats (the so-called RR interval) tends to depend linearly on the amplitude of heart beat. It is thus valuable to explore the possibility of utilising our model to understand heart rate variability and its implication for healthy heart. This issue will be investigated in future publication.

---

[1] W. B. Cannon, "Organization for physical homeostasis", Physiological Rev. **9**, 399–431 (1929).

[2] The biology of cancer, R. A. Weinberg, 2nd Ed., Garland Science (2014).

[3] Medical physiology, W. F. Boron and L. Boulpaep, Rev. Ed., Saunders (2004).

[4] H. Haken, Information and Self-organization: A macroscopic approach to complex systems, 3rd Ed., Springer, p.63-64 (2006).

[5] A.P.L. Newton, E. Kim and H.-L. Liu, "On the self-organizing process of large scale shear flows", Phys. Plasmas, **20**, 092306 (2013).

[6] E. Kim, H. Liu and J. Anderson, "Probability distribution function for self-organization of shear flows", Phys. Plasmas, **16**, 0552304 (2009).

[7] E. Kim and P.H. Diamond, "Zonal flows and transient dynamics of the L-H transition", Phys. Rev. Lett., **90**, 185006 (2003).

[8] E. Kim, "Consistent theory of turbulent transport in two dimensional magnetohydrodynamics", Phys. Rev. Lett., **96**, 084504 (2006).

[9] A.P. Feinberg and R.A. Irizarry RA, "Stochastic epigenetic variation as a driving force of development, evolutionary adaptation, and disease", Proceedings of National Academy of Sciences of the United States of America, **107**, 1757–1764 (2010).

[10] N.X. Wang, X.M. Zhang, X.B. Han, "The effects of environmental disturbances on tumor growth", Brazilian Journal of Physics, **42**, 253–260 (2012).

[11] J. Lee, K. S. Farquhar, J. Yun, C. Frankenberger, E. Bevilacqua, K. Yeung, E. Kim, G. Balázsi and M. R. Rosner, "Network of mutually repressive metastasis regulators can promote cell heterogeneity and metastatic transitions", Proceedings of National Academy of Sciences of the United States of America, **111(3)**, E364–E373 (2014).

[12] U. Lee, J. J. Skinner, J. Reinitz, M. R. Rosner, and E. Kim, "Noise-driven phenotypic heterogeneity with finite correlation time", PLoS One, **10(7)**, e0132397 (2015).

[13] A. d'Onofrio, "Fractal growth of tumors and other cellular populations: linking the mechanistic to the phenomenological modeling and vice versa", Chaos, Solitons, and Fractals, **41**, 875–880 (2009).

[14] B. van der Pol, "On relaxation-oscillations", The London, Edinburgh, and Dublin Phil. Mag.

and J. Sci. Ser.7, **2**, 978–992 (1926).

[15] B. van der Pol, "Forced oscillations in a circuit with non-linear resistance (reception with reactive triode)", The London, Edinburgh, and Dublin Phil. Mag. J. Sci. Ser.7, **3**, 65–80, (1927).

[16] B. van der Pol and J. van der Mark, "Frequency demultiplication", Nature, **120**, 363–364 (1927).

[17] B. van der Pol and J. van der Mark, "The heartbeat considered as a relaxation oscillation, and an electrical model of the heart", The London, Edinburgh, and Dublin Phil. Mag. J. Sci. Ser.7, **6**, 763–775 (1928).

[18] S. R.F.S.M. Gois and M.A. Savi, "An analysis of heart rhythm dynamics using a three-coupled oscillator model", Chaos, Solitons & Fractals, **41**, 2553–2565 (2009).

[19] R.R. Alieve and A. V. Panvilov, "A Simple Two-variable Model of Cardiac Excitation, Chaos, Solitons & Fractals", **7**, 293–301 (1996).

[20] C.R. Katholi, F. Urthaler, J. Macy, Jr., and T.N. James, "A Mathematical Model of Automaticity in the Sinus Node and AV Junction Based on Weakly Coupled Relaxation oscillators", Comp. Biomed. Res, **10**, 529–543 (1977).

[21] J. J. Zebrowski, K. Grudzińki, T. Buchner, P. Kuklik, J. Gac, G. Gielerak, P. Sanders, and R. Baranowski, "Nonlinear oscillator model reproducing various phenomena in the dynamics of the conduction system of the heart", Chaos, **7**, 015121 (2007).

[22] B. J. West, A. L. Goldberger, G. Rovner, and V. Bhargava, "Nonlinear dynamics of the heartbeat. I. The AV junction: Passive conduit or active oscillator?", Physica D, **17**, 198–206 (1985).

[23] K. Grudziński and J. J. Źebrowski, "Modeling cardiac pacemakers with relaxation oscillators", Physica A, **336,** 153–162 (2004).

[24] E. Ryzhii and M. Ryzhii, "A heterogeneous coupled oscillator model for simulation of ECG signals", Comp. Meth. Programs Biomed., **117**, 40–49 (2014).

[25] L. Glass and M.C. Mackey, From Clocks to Chaos. The Rhythms of Life (Princeton University Press, Princeton, 1988); H.G. Schuster, Deterministic Chaos: An Introduction (VCH, Weinheim, 1988); W.-B. Zhang, Synergetic Economics (Springer-Verlag, Berlin Heidelberg, 1991); V.S. Anishchenko, Dynamical Chaos Models and Experiments (World Scientific, Singapore,1995); H.D.I. Abarbanel, M.I. Rabinovich, A. Selverston, M.V. Bazhenov, R. Huerta,

M.M. Sushchik, and L.L.Rubchinskii, “Synchronization in neural networks”, Phys. Usp., **39**, 337–362 (1996).

[26] M. Gitterman, “Underdamped oscillator with fluctuating damping”, J. Phys. A: Math. Gen. **37**, 5729–5736 (2004); M. Gitterman, The noisy oscillator, random mass, frequency, damping. 2nd Ed., World Sci. Pub. Co. Pte. Ltd. (2013).

[27] U. Parlitz and W. Lauterborn, “Period–doubling cascades and devil’s staircases of the driven Van der Pol oscillator”, Phys. Rev. A. **36**, 1428-1434 (1987).

[28] Z. Qu, G. Hu, A. Garfinkel and J.N. Weiss, “Nonlinear and stochastic dynamics in the heart”, Phys. Rep., **543**, 61-162 (2014).

[29] M.C. Teich, S.B. Lowen, B.M. Jost, and K. Vibe-Rheymer, “Heart rate variability: measures and models”, arxiv.org/abs/physics/0008016v1

[30] T. Costa, G. Boccignone, and M. Ferraro, “Gaussian mixture model of heart rate variability”, PLoS One, **7**, e37731 (2012).

[31] Task Force of The European Society of Cardiology and The North American Society of Pacing and Electrophysiology: Standards of measurement, physiological interpretation, and clinical use, Euro. Heart J. **17**, 354-381 (1996).

[32] H. Gothwa, S. Kedawat, and R. Kumar, “Cardiac arrhythmias detection in an ECG beat signal using fast fourier transform and artificial neural network”, J. Biomed. Sci. and Eng., **4**, 289-296 (2011).

[33] D. A. Siders and D. Moulopoulos, “Mechanism of atrioventricular conduction: study on an analogue”, Elrctrocardiology, **10**, 51-58 (1977).

[34] N. Weiss, Z. Qu, P.-S. Chen, S.-F. Lin, H.S. Karagueuzian, H. Hayashi, A. Garfinkel and A. Karma, “The dynamics of cardiac fibrillation”, Circulation, **112**, 1232-1240 (2005).

[35] To be specific, for small $x < \sqrt{\alpha/\beta}$, $-\alpha + \beta x^2$ is negative leading to the growth of x while for large $x > \sqrt{\alpha/\beta}$, $-\alpha + \beta x^2$ becomes positive, causing damping of x.

[36] The signs of ϵ_1 and ϵ_2 do not affect our results.

[37] Note that effect of fluctuation in damping parameter tends to be more robust compared to that in fluctuation in oscillation frequency ω_0. For instance, the previous study [26] has shown that random (Gaussian) fluctuation μ_1 can give rise to the growth of the first moment (e.g. the average x), in contrast to the case of random frequency whose effect appears in higher order moment (e.g. $\langle x^2 \rangle$).

[38] For sufficiently large $\epsilon_1 \geq 4$, it is possible that the second mode of frequency $p_B = \sqrt{2} + 1$ (which requires $\epsilon_1 \geq 4$) could be contributing to frequency locking, etc.

[39] Similar change in limit cycle was previously shown in the forced Van der Pol oscillator with an additive oscillatory forcing [27].